Throughput Optimization in Adaptive Transmit Antenna Selection Systems With Limited Feedback

Tong Wu, Yulong Zou, Jia Zhu, Hao Wei, and George K. Karagiannidis, *Fellow, IEEE*

***Abstract*—We investigate the performance of a downlink wireless system with a multiantenna base station under the effect of limited channel feedback. In order to inactivate transmit antennas with poor channel quality and, thus, reduce the feedback overhead, a channel gain threshold-based multiantenna selection (CGT-MAS) scheme is proposed without optimization (NOCGT-MAS) and the corresponding single-antenna scheme (NOCGT-SAS) is considered as a baseline. Considering that the number of selected antennas affects both data transmission rate and the feedback overhead, an effective throughput defined as the difference between the data transmission rate and feedback rate is employed for evaluating the system performance. We conduct an effective throughput analysis for both the NOCGT-SAS and NOCGT-MAS schemes and show that an optimal channel gain threshold exists to maximize the effective throughput of the proposed NOCGT-MAS scheme. As a consequence, we propose the optimal instantaneous CGT-MAS algorithm (OICGT-MAS) to maximize the instantaneous effective throughput. Besides, we derive a closed-form expression of an average effective throughput for the CGT-MAS scheme and propose an optimal average channel gain threshold-based multiantenna selection algorithm (OACGT-MAS) for maximizing the derived average effective throughput. Numerical results demonstrate that the effective throughput of the proposed NOCGT-MAS is substantially better than that of conventional NOCGT-SAS. Moreover, although the OICGT-MAS scheme has a slight advantage over OACGT-MAS in terms of the effective throughput, it has a much higher computational complexity than the latter method.**

***Index Terms*—Adaptive transmit antenna selection, channel gain threshold, channel quantization, effective throughput, limited feedback.**

I. Introduction

AIMING at improving the communication quality, and expanding the channel capacity without increasing the spectrum resources and the transmit power, multiantenna has been widely discussed and concerned in recent years [1]–[4]. Due to the higher array gain and diversity gain comparing with single-antenna system [5], the application of multiantenna technology can achieve better system performance for many different types of wireless communication systems, such as cellular networks [6], multirelay networks [7]–[9], cognitive wireless networks [10], [11], as well as heterogeneous networks [12]. As a hot topic, multiantenna technology realizes the substantial enhancement of the wireless communication performance. However, it also has many defects at the same time, since that the feedback circuit loss, power consumption, and hardware cost all have greatly increased as the number of antenna channels increases in multiple antenna technology, causing the improvement of system energy consumption and further reducing the system effective transmission performance.

A. Prior Work

To reduce the system complexity and the hardware costs of multiantenna system, transmit antenna selection (TAS) scheme has been widely concerned [13]–[21], where only partial antennas are selected through various selection criteria to be active in transmitting signals. Besides the TAS based on selection combining (TAS/SC) scheme [13] and TAS scheme with maximal ratio combining (TAS/MRC) [14], [15] at the receiver, a generalized selection combining scheme for TAS (TAS/GSC) [16] is proposed, which not only can reduce the complexity compared with TAS/SC but also can improve the performance compared with TAS/MRC. Further, TAS with switch-and-examine combining (TAS/SEC) [17] and SEC with post-selection (TAS/SECPS) [18] are proposed to reduce the complexity for small mobile units. To improve the performance of TAS/GSC scheme, the TAS/GSC with optimal threshold (TAS/OT-GSC) is proposed in [19], which can achieve similar symbol error rate (SER) performance with less number of channel estimation as compared with the TAS/GSC by optimizing the predetermined signal-to-noise ratio (SNR) threshold. Additionally, there are some other TAS schemes. A new threshold-based selection scheme is proposed in [20] to decrease the system complexity according to the Markov chain theory. The research develops an optimal TAS rule in [21] for minimizing the average symbol error probability of a cognitive relay network.

On the other hand, considering that the quantized channel state information (CSI) is accord with the reality of the limited resources, many researchers concentrate on the enhancement of the system performance with limited feedback [22]–[27]. Zhang and Cheng [22] maximize the capacity by setting an optimal power gain threshold for a cooperative relay system with limited feedback. The system performance metrics, including outage probability and so on, of three different TAS schemes are studied in [23] with limited feedback. In order to maximize

Manuscript received 16 July 2021; revised 31 October 2021 and 5 January 2022; accepted 20 January 2022. Date of publication 17 February 2022; date of current version 9 December 2022. This work was supported in part by the National Natural Science Foundation of China under Grant 62071253 and in part by the Postgraduate Research and Practice Innovation Program of Jiangsu Province under Grant KYCX20_0734. *(Corresponding author: Yulong Zou.)*

Tong Wu, Yulong Zou, and Jia Zhu are with the School of Telecommunications and Information Engineering, Nanjing University of Posts and Telecommunications, Nanjing 210003, China (e-mail: wutong19941101@163.com; yulong.zou@njupt.edu.cn; jiazhu@njupt.edu.cn).

Hao Wei is with the State Key Laboratory of Mobile Network and Mobile Multimedia Technology, ZTE Corporation, Shenzhen 518055, China (e-mail: weihao@seu.edu.cn).

George K. Karagiannidis is with the Department of Electrical and Computer Engineering, Aristotle University of Thessaloniki, 54124 Thessaloniki, Greece (e-mail: geokarag@auth.gr).

Digital Object Identifier 10.1109/JSYST.2022.3148089

the net spectral efficiency, a tight lower bound on the optimum number of feedback bits for a downlink multiantenna cellular network is found in [24]. A close estimate of the optimal number of feedback bits is proposed in [25] for a multiantenna cellular network with limited feedback. Considering the effect of limited feedback frame work, the design, performance analysis, and optimization of a nonorthogonal multiple access multiantenna system are provided in [26]. Two novel reduced feedback rate TAS schemes for the multiple-input single-output (MISO) systems are proposed and analyzed in [27].

B. Motivation

To the best of our knowledge, there are rarely prior researches on the effects of the multiantenna selection (MAS) scheme considering limited feedback on the effective throughput, which is defined to take both data transmission rate and feedback overhead into account. Most current research efforts of TAS scheme are devoted to single-antenna selection, where only one optimal transmit is employed for signal transmission [13]–[21], [23]. Nevertheless, there are some studies that concentrate on multiple TAS scheme [22] and [28]. However, these studies lack the consideration of the adverse effect of the feedback overhead. Besides, the schemes proposed in [24], [25], and our previous work [1], [29], take the adverse effect of channel quantization error into consideration, but are lack of the employment of TAS scheme. Both TAS scheme and feedback overhead are taken into account in [27], but the TAS scheme only optimized with fixed number of active antennas without adaptation. Motivated by these, we investigate the performance of a wireless system consisting of a multiantenna base station and a single-antenna user based on the channel gain threshold-based multiantenna selection (CGT-MAS) scheme in face of limited feedback in this article, taking both MAS scheme and limited feedback into consideration.

C. Our Contributions

Our main contributions are listed as follows.

1) We propose a CGT-MAS scheme without optimization (NOCGT-MAS) for our multiantenna network, where partial transmit antennas with good quality can be employed by setting the channel gain threshold, to mitigate the adverse impacts of limited feedback since that the number of selected antennas affects not only the data transmission rate but also the feedback rate. Meanwhile, the corresponding single-antenna selection (NOCGT-SAS) scheme is considered as a baseline, where only the optimal antenna with the largest channel gain exceeding the threshold can be employed for transmission.
2) In order to evaluate the system transmission performance, we define the effective throughput as the difference between the data transmission rate and the feedback rate, taking both transmission and feedback into consideration. We present an effective throughput analysis for both NOCGT-SAS and NOCGT-MAS schemes, showing that there exists an optimal channel gain threshold which can maximize the effective throughput of proposed NOCGT-MAS scheme. Numerical results demonstrate that the effective throughput performance of our proposed NOCGT-MAS is better than that of conventional NOCGT-SAS.
3) We construct the optimization problem of the channel gain threshold. We propose the optimal instantaneous CGT-MAS (OICGT-MAS) iterative algorithm for the sake of maximizing the instantaneous effective throughput. We derive a closed-form expression of an average effective throughput for the CGT-MAS scheme and propose an optimal average CGT-MAS (OACGT-MAS) algorithm for maximizing the derived average effective throughput. Simulation results indicate that, in terms of effective throughput, the OICGT-MAS outperforms the OACGT-MAS at the cost of computational complexity.

The remainder of this article is organized as follows. In Section II, we illustrate the system model. In Section III, we describe the system effective transmission performance through effective throughput for both NOCGT-SAS scheme and NOCGT-MAS scheme. In Section IV, we construct the optimization problem for NOCGT-MAS scheme, provide the derivation of the closed-form average effective throughput expression, and propose two iterative algorithms called OICGT-MAS and OACGT-MAS as the solutions. Section V presents numerical results and discussion about the effective throughput. The conclusion is driven in Section VI.

II. System Model

In this article, we consider a basic downlink MISO wireless system containing a base station as the source equipped with M ($M \geq 2$) antennas, and a single-antenna user as the destination. Such kind of system can be widely applied to other scenarios, including heterogeneous cellular networks and UAV communication systems, since that either multiple centralized or distributed antennas can be employed for improving system performance. Multiple user scheduling scheme for a downlink multi-antenna network will be investigated for our future work. Assuming that the CSI is available at the destination, while the source acquires CSI by limited feedback, the channel coefficients at the source are quantized values denoted by $\hat{h}_{id}$ ($i = 1, 2, \ldots, M$), where i represents the index of the ith antenna A_i at the source. It is worth noting that the research in this article focuses on the impact of limited feedback on system performance without considering channel estimation errors, but similar conclusions will be obtained when the estimation error is considered, which is also left for our future work. Consequently, the real channel coefficients can be rewritten as

$$h_{id} = \hat{h}_{id} - h_{ie} \tag{1}$$

where h_{id} represents the real Rayleigh fading channel coefficient from the ith antenna at the source to the destination, with zero mean and variance σ_{id}^2, and h_{ie} is the quantization error of ith channel coefficient, modeled as the complex Gaussian random variables (RVs) with zero mean. Moreover, both h_{id} and h_{ie} for different antennas are independent distributed.

Next, the equal probability quantization (EPQ) method is employed for quantizing both the real and imaginary parts of channel coefficients, where the total probability is equally divided into $N_q = 2^{N_c/2}$ quantization steps, since total quantization bits for one channel N_c are allocated equally to the real and imaginary parts. As shown in [1] and [29], the lth quantization level d_l can be expressed as

$$d_l = \frac{\sigma_{id}}{\sqrt{2}} Q^{-1}\left(1 - \frac{l}{N_q}\right), l \in \{0, 1, \ldots, N_q\} \tag{2}$$

where

$$Q(x) = \int_x^{\infty} \frac{1}{\sqrt{2\pi}} \exp\left(-\frac{1}{2}t^2\right) dt \tag{3}$$

$Q^{-1}(x)$ represents an inverse function of $Q(x)$. Meanwhile, the lth quantized value q_l can be expressed as

$$q_l = \frac{\sigma_{id}}{\sqrt{2}} Q^{-1}\left(1 - \frac{2l-1}{N_q}\right), l \in \{1, \ldots, N_q\} \tag{4}$$

and the variance of h_{ie} is given by $\sigma_{ie}^2 = 2\sum_{l=1}^{N_q} \Phi_l$, where

$$\begin{aligned}\Phi_l = &\left(\frac{\sigma_{id}^2}{2} + q_l^2\right)\left[Q\left(\frac{\sqrt{2}d_{l-1}}{\sigma_{id}}\right) - Q\left(\frac{\sqrt{2}d_l}{\sigma_{id}}\right)\right] \\ &+ \frac{\sigma}{2\sqrt{\pi}}\left[(2q_l - d_l)\exp\left(-\frac{d_l^2}{\sigma_{id}^2}\right)\right. \\ &\left. - (2q_l - d_{l-1})\exp\left(-\frac{d_{l-1}^2}{\sigma_{id}^2}\right)\right].\end{aligned} \tag{5}$$

The derivations of (2), (4), and (5) are shown in Appendix A.

It should be pointed out that the emphasis in this work is the system performance enhancement of our proposed NOCGT-MAS scheme compared with conventional NOCGT-SAS scheme. Hence, the random vector quantization (RVQ) and other quantization methods can also be used in our proposed NOCGT-MAS scheme. In order to show that different quantization methods do not affect the advantage of our proposed NOCGT-MAS scheme, the results of RVQ-based NOCGT-MAS and NOCGT-SAS schemes will be given in Section III. The simpler implementation of EPQ method accounts for the replacement of RVQ. We only need to feedback the quantized value in EPQ, while many different predesigned codebooks have to be synchronized between the source and destination in RVQ method since that the predesigned codebook for different number of selected antennas is different.

We set a threshold α ($\alpha \geq 0$) to select antennas employed for transmitting signal, while the antennas whose channel gain $|h_{id}|^2$ fail to exceed α are inactivated. Hence, only the CSI from those selected channels can be quantized and fed back to source, which further decreases the feedback overhead related to the number of active antennas at source.

For the reader convenience, let $\mathcal{T}$ represent the transmission set of antennas that can be used to transmit signal x_s. Then, $|\mathcal{T}|$ ($0 \leq |\mathcal{T}| \leq M$) antennas at $\mathcal{T}$, which satisfy the criterion of RVs $|h_{id}|^2$, can be employed for transmitting the same signal x_s with total transmit power P_s to the destination, where $|\mathcal{T}|$ represents the cardinality of the set $\mathcal{T}$, $E(|x_s|^2) = P_s$ and $E(\cdot)$ denotes the statistical average operator. Based on the description above, the criterion can be expressed as

$$|h_{id}|^2 > \alpha, A_i \in \mathcal{T}. \tag{6}$$

Given M antennas at source, there are 2^M possible subsets $\mathcal{T}$, then the sample space of $\mathcal{T}$ can be formulated as

$$\Omega = \{\phi, \mathcal{T}_1, \mathcal{T}_2, \ldots, \mathcal{T}_n, \ldots, \mathcal{T}_{2^M-1}\} \tag{7}$$

where ϕ represents the empty set and $\mathcal{T}_n$ represents the nth nonempty transmission subset of $|\mathcal{T}_n|$ antennas. If the set $\mathcal{T}$ is empty, which means that no RV $|h_{id}|^2$ exceeds the threshold, no antenna is employed for transmitting the signal x_s in this case. If the set $\mathcal{T}$ is nonempty, there will be some antenna channels that can be used to transmit signal x_s from the source to the destination.

III. Effective Throughput Analysis

In this section, we analyze the effective throughput performance for both NOCGT-SAS scheme and NOCGT-MAS scheme over Rayleigh fading channels.

A. Conventional NOCGT-SAS Scheme

In this subsection, we concentrate on the signal transmission model for the NOCGT-SAS scheme. For NOCGT-SAS scheme, only the optimal antenna with maximal real channel gain will have the chance to transmit signal. Accordingly, the optimal antenna selection criterion can be written as

$$h_{sd} = \arg \max_{1 \leq i \leq M} |h_{id}|^2 \tag{8}$$

where h_{sd} represents real channel coefficient of the optimal transmit antenna.

It is assumed that the optimal antenna will be selected when its channel gain exceeds the threshold, and the index of the selected antenna will be fed back to the source. Otherwise, no antenna is employed and no CSI is fed back.

Consequently, the received signal at the destination can be given by

$$y_d^{\text{SAS}} = \begin{cases} h_{sd}x_s + n_d, & |h_{sd}|^2 > \alpha \\ n_d, & |h_{sd}|^2 \leq \alpha \end{cases} \tag{9}$$

where n_d is the zero-mean complex additive white Gaussian noise (AWGN) with the variance N_0.

To the end, the data transmission rate of the CGT-SAS scheme can be written as

$$C_d^{\text{SAS}} = \begin{cases} B_c \log_2\left(1 + \gamma_s |h_{sd}|^2\right), & |h_{sd}|^2 > \alpha \\ 0, & |h_{sd}|^2 \leq \alpha \end{cases} \tag{10}$$

where B_c is the bandwidth, and $\gamma_s = \frac{P_s}{N_0}$ represents the SNR.

Despite that the quantized CSI does not need to be used in the precoding design at source in NOCGT-SAS scheme, there still needs $\log_2(M)$ bits to feed back the index of the selected antenna to the source to indicate which antenna is employed for transmission, since there are M antennas at source. Meanwhile, if no antenna is selected, there is no feedback. Hence, learning from Refs. [1] and [24], the feedback rate can be presented as

$$C_F^{\text{SAS}} = \begin{cases} \frac{\log_2 M}{T_c}, & |h_{sd}|^2 > \alpha \\ 0, & |h_{sd}|^2 \leq \alpha \end{cases} \tag{11}$$

where T_c represents the coherence time.

Combining (10) and (11), we can express the effective throughput of NOCGT-SAS scheme according to (32) from our previous work [1] as

$$\begin{aligned} C_T^{\text{SAS}} &= C_d^{\text{SAS}} - C_F^{\text{SAS}} \\ &= \begin{cases} B_c \log_2\left(1 + \gamma_s |h_{sd}|^2\right) - \frac{\log_2 M}{T_c}, & |h_{sd}|^2 > \alpha \\ 0, & |h_{sd}|^2 \leq \alpha. \end{cases} \end{aligned} \tag{12}$$

B. Proposed NOCGT-MAS Scheme

In this subsection, we describe the signal transmission of the NOCGT-MAS scheme, where antennas in the transmit set $\mathcal{T}$

are all employed for transmitting signal from the source to the destination.

According to the description in Section II, when $\mathcal{T} = \phi$, there is no antenna to be used for transmitting signal. When $|\mathcal{T}_n| = 1$, the received signal at destination is similar as that of NOCGT-SAS scheme. When $|\mathcal{T}_n| > 1$, there exists more than one antenna to be employed for transmission. Hence, the quantized CSI needs to be fed back to the source for precoding design. Denote $\mathbf{w} = [w_1, w_2, \ldots, w_{|\mathcal{T}_n|}]^T$ as the normalized precoding vector, where $\sum_{i=1}^{|\mathcal{T}_n|} |w_i|^2 = 1$. Thus, the signal received by the destination can be expressed as

$$y_d^{\text{MAS}} = \begin{cases} \sum\limits_{A_i \in \mathcal{T}_n} w_i h_{id} x_s + n_d, & |\mathcal{T}_n| > 1 \\ h_{sd} x_s + n_d, & |\mathcal{T}_n| = 1 \\ n_d, & \mathcal{T} = \phi. \end{cases} \tag{13}$$

Substituting (1) into (13) yields

$$y_d^{\text{MAS}} = \begin{cases} \sum\limits_{A_i \in \mathcal{T}_n} w_i (\hat{h}_{id} - h_{ie}) x_s + n_d, & |\mathcal{T}_n| > 1 \\ h_{sd} x_s + n_d, & |\mathcal{T}_n| = 1 \\ n_d, & \mathcal{T} = \phi. \end{cases} \tag{14}$$

From a worst perspective of design, we could treat the quantization interference as Gaussian-distributed RVs. Nevertheless, it is of great interest to explore how to intelligently utilize the well-known CSI at destination to reduce the quantization interference for our future work. Thus, data transmission rate of the NOCGT-MAS scheme is given by

$$C_d^{\text{MAS}} = \begin{cases} B_c \log_2 \left(1 + \frac{\gamma_s |\sum\limits_{A_i \in \mathcal{T}_n} w_i \hat{h}_{id}|^2}{E_{md}+1} \right), & |\mathcal{T}_n| > 1 \\ B_c \log_2 \left(1 + \gamma_s |h_{sd}|^2 \right), & |\mathcal{T}_n| = 1 \\ 0, & \mathcal{T} = \phi \end{cases} \tag{15}$$

where E_{md} is the expectation of an unknown quantization error vector. Denote $\mathbf{h}_e = [h_{1e}, h_{2e}, \ldots, h_{|\mathcal{T}_n|e}]^T$ as the unknown quantization error vector. We can represent E_{md} from (15) as

$$\begin{aligned} E_{md} &= E(\gamma_s |\sum_{A_i \in \mathcal{T}_n} w_i h_{ie}|^2) \\ &= \gamma_s E(\mathbf{w}^H \mathbf{h}_e^* \mathbf{h}_e^T \mathbf{w}) \\ &= \gamma_s \sum_{A_i \in \mathcal{T}_n} |w_i|^2 \sigma_{ie}^2. \end{aligned} \tag{16}$$

According to (22) from [30], the optimal w_i of maximal ratio transmission is given by $w_i^{\text{opt}} = \frac{\hat{h}_{id}^*}{\sqrt{\sum_{A_i \in \mathcal{T}_n} |\hat{h}_{id}|^2}}$.

Substituting w_i^{opt} into (16), the expectation of the unknown quantization error vector is changed into

$$E_{md} = \gamma_s \frac{\sum\limits_{A_i \in \mathcal{T}_n} |\hat{h}_{id}|^2 \sigma_{ie}^2}{\sum\limits_{A_i \in \mathcal{T}_n} |\hat{h}_{id}|^2} \tag{17}$$

and the data transmission rate from (15) is turned into

$$C_d^{\text{MAS}} = \begin{cases} B_c \log_2 \left(1 + \frac{\gamma_s \sum\limits_{A_i \in \mathcal{T}_n} |\hat{h}_{id}|^2}{E_{md}+1} \right), & |\mathcal{T}_n| > 1 \\ B_c \log_2 \left(1 + \gamma_s |h_{sd}|^2 \right), & |\mathcal{T}_n| = 1 \\ 0, & \mathcal{T} = \phi. \end{cases} \tag{18}$$

As for the feedback model of NOCGT-MAS scheme, there are three cases mentioned as follows. i) When $\mathcal{T} = \phi$, no CSI needs to be fed back. ii) When $|\mathcal{T}_n| = 1$, the feedback needs 1 bit to inform the source that only one antenna is selected. In this case, there are M possible transmission subsets and no CSI needs to be quantized. Therefore, the total number of feedback bits is $\log_2 M + 1$. iii) When $|\mathcal{T}_n| > 1$, the feedback also needs 1 bit to inform the case that more than one antenna are selected. In this case, there are $2^M - 1 - M$ possible transmission subsets. Meanwhile, $|\mathcal{T}_n| N_c$ bits are needed to quantize CSI for the precoding design, where N_c represents the number of quantization bits per channel. Consequently, a total of $|\mathcal{T}_n| N_c + \log_2(2^M - 1 - M) + 1$ bits are required for the feedback. Then, the feedback rate of NOCGT-MAS scheme can be written as

$$C_F^{\text{MAS}} = \begin{cases} \frac{|\mathcal{T}_n| N_c + \log_2(2^M - 1 - M) + 1}{T_c}, & |\mathcal{T}_n| > 1 \\ \frac{\log_2 M + 1}{T_c}, & |\mathcal{T}_n| = 1 \\ 0, & \mathcal{T} = \phi. \end{cases} \tag{19}$$

Accordingly, the effective throughput of NOCGT-MAS scheme can be presented as (20) shown at bottom of the page.

It can be observed from (20) that, when γ_s is in a high region, the effective throughput in case $|\mathcal{T}_n| > 1$ can reach an asymptotic floor, which can be further expressed as

$$\begin{aligned} C_T^{\text{MAS}}(|\mathcal{T}_n| > 1) = B_c \log_2 &\left[1 + \frac{(\sum\limits_{A_i \in \mathcal{T}_n} |\hat{h}_{id}|^2)^2}{\sum\limits_{A_i \in \mathcal{T}_n} |\hat{h}_{id}|^2 \sigma_{ie}^2} \right] \\ &- \frac{|\mathcal{T}_n| N_c + \log_2(2^M - 1 - M) + 1}{T_c}. \end{aligned} \tag{21}$$

By employing (21), we provide the results of asymptotic simulation in Fig. 5 to show the asymptotic floor of NOCGT-MAS scheme with high SNR.

For the purpose of illustrating that different quantization methods do not have much effect on the trends of the effective

$$C_T^{\text{MAS}} = C_d^{\text{MAS}} - C_F^{\text{MAS}} = \begin{cases} B_c \log_2 \left(1 + \frac{\gamma_s \sum\limits_{A_i \in \mathcal{T}_n} |\hat{h}_{id}|^2}{E_{md}+1} \right) - \frac{|\mathcal{T}_n| N_c + \log_2(2^M - 1 - M) + 1}{T_c}, & |\mathcal{T}_n| > 1 \\ B_c \log_2 \left(1 + \gamma_s |h_{sd}|^2 \right) - \frac{\log_2 M + 1}{T_c}, & |\mathcal{T}_n| = 1 \\ 0, & \mathcal{T} = \phi \end{cases} \tag{20}$$

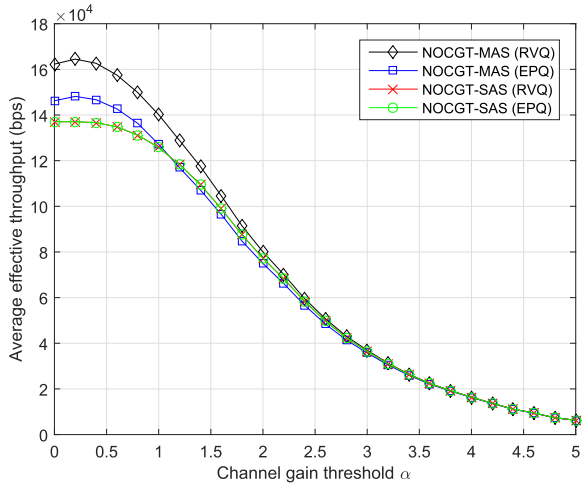

Fig. 1. Average effective throughput versus channel gain threshold α of NOCGT-MAS and NOCGT-SAS schemes for the RVQ and EPQ quantization methods, with the bandwidth $B_c = 70$ kHz, the coherence time $T_c = 1$ ms, the number of total transmit antennas $M = 4$, the number of feedback bits per channel $N_c = 6$, the SNR $\gamma_s = 2$ dB, and the channel gain $\sigma_{id}^2 = 1$.

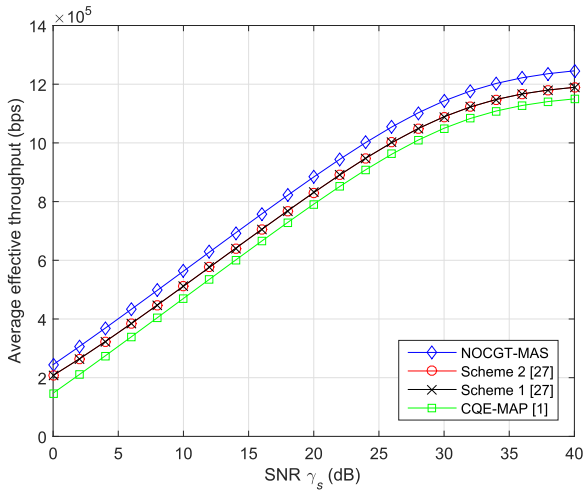

Fig. 2. Average effective throughput versus SNR of the NOCGT-MAS scheme, two existing TAS schemes in [27] and CQE-MAP scheme in [1] with the bandwidth $B_c = 100$ kHz, the coherence time $T_c = 1$ ms, the number of total transmit antennas $M = 16$, the number of feedback bits per channel $N_c = 16$, and the channel gain $\sigma_{id}^2 = 1$.

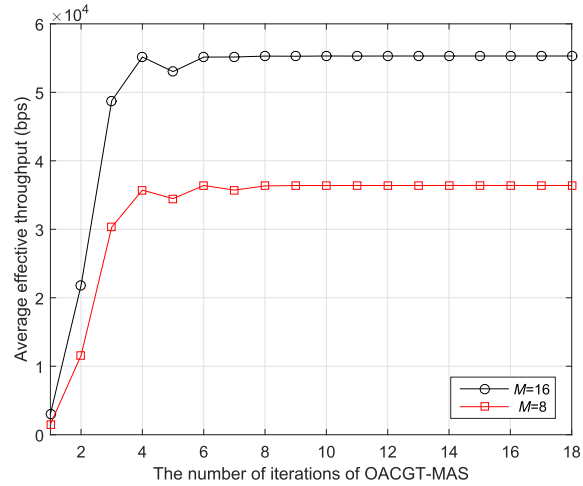

Fig. 3. Average effective throughput versus the number of iterations of OACGT-MAS with the bandwidth $B_c = 120$ MHz, the coherence time $T_c = 1$ ms, the number of total transmit antennas $M = 16$, the number of feedback bits per channel $N_c = 24$, the SNR $\gamma_s = -40$ dB, and the channel gain $\sigma_{id}^2 = 1$.

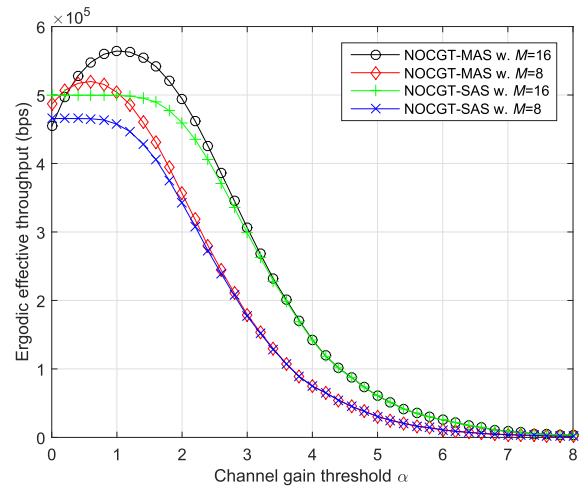

Fig. 4. Average effective throughput versus channel gain threshold α of NOCGT-MAS and NOCGT-SAS schemes for different number of total transmit antennas M with the bandwidth $B_c = 100$ kHz, the number of quantization bits per channel $N_c = 16$, the SNR $\gamma_s = 10$ dB, and the channel gain $\sigma_{id}^2 = 1$.

throughput for both NOCGT-MAS scheme and NOCGT-SAS scheme, we provide the simulation results for both RVQ and EPQ methods in Fig. 1. It can be observed that the average effective throughput of the NOCGT-SAS for both RVQ and EPQ methods is the same since that the NOCGT-SAS scheme does not need the quantized CSI. Besides, the trends of effective throughput curves of NOCGT-MAS scheme for both RVQ and EPQ methods are the same. Specifically, as α increases, effective throughput curves of RVQ- and EPQ-based NOCGT-MAS schemes both increase first and then decrease. This is because that the fading speed of data transmission rate gradually changes from lower to higher than that of feedback overhead as α increases. Accordingly, there exists an optimal effective throughput of NOCGT-MAS scheme. The detailed introduction to the optimization problem will be given in Section IV. Moreover, it also can be observed that the performance of NOCGT-MAS scheme is better than or the same as that of NOCGT-SAS scheme in most cases, showing the advantage of NOCGT-MAS scheme. However, sometimes the performance of NOCGT-MAS scheme is slightly worse than that of NOCGT-SAS scheme with EPQ methods. This is because that, when the number of active antennas in NOCGT-MAS scheme is not much more than that in NOCGT-SAS scheme, the existence of quantization error makes the advantage of transmission rate slightly lower than the disadvantage of feedback rate of NOCGT-MAS over NOCGT-SAS, resulting in the slightly

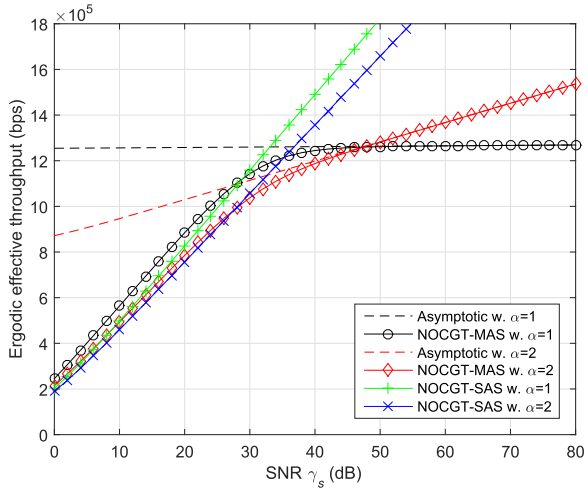

Fig. 5. Average effective throughput versus SNR γ_s of NOCGT-MAS and NOCGT-SAS schemes for different channel gain threshold α with the bandwidth $B_c = 100$ kHz, the number of total transmit antennas $M = 16$, the number of quantization bits per channel $N_c = 16$, and the channel gain $\sigma_{id}^2 = 1$.

worse performance. When N_c is a sufficiently large value, our proposed NOCGT-MAS scheme can always achieve a better performance than NOCGT-SAS scheme with EPQ methods, which is shown in Fig. 4 in Section V.

In order to further show the advantage of our proposed NOCGT-MAS scheme, we provide the simulation results of our proposed NOCGT-MAS scheme, two existing TAS schemes in [27] where the antennas are selected by different manners, and the channel quantization errors-oriented multiantenna precoding (CQE-MAP) scheme proposed in our previous work [1] without TAS. Fig. 2 illustrates the average effective throughput versus SNR of the NOCGT-MAS scheme with $\alpha = 1$, two existing TAS schemes in [27], and CQE-MAP scheme in [1]. It can be observed from Fig. 2 that, our proposed NOCGT-MAS scheme performs best, two existing TAS schemes perform similar, and CQE-MAP scheme without TAS performs worst, further confirming the advantage of our proposed scheme. Besides, it also can be seen from Fig. 2 that, with the growth of SNR, the average effective throughput of these four schemes all converge to their respective floors, due to the interference caused by channel quantization.

IV. Effective Throughput Maximization

In this section, we concentrate on the maximization of the effective throughput for NOCGT-MAS scheme and provide two iterative algorithms as the solutions.

For simplicity, similar to [30], we assume that the RVs h_{id} are independent and identically distributed (i.i.d.), which means that they have the same variance denoted by σ_d^2. We also can conclude that when the RVs h_{ie} are i.i.d., they have the same variance represented by σ_e^2. To this end, the expectation of the unknown quantization error vector given by (17) in NOCGT-MAS scheme can be simplified as

$$E_{md} = \gamma_s \sigma_e^2. \tag{22}$$

Then, substituting (22) into (18), the C_d^{MAS} can be further expressed as

$$C_d^{\text{MAS}} = \begin{cases} B_c \log_2\left(1 + \frac{\gamma_s \sum\limits_{A_i \in \mathcal{T}_n} |\hat{h}_{id}|^2}{\gamma_s \sigma_e^2 + 1}\right), & |\mathcal{T}_n| > 1 \\ B_c \log_2\left(1 + \gamma_s |h_{sd}|^2\right), & |\mathcal{T}_n| = 1 \\ 0, & \mathcal{T} = \phi. \end{cases} \tag{23}$$

Considering that number of selected antennas $|\mathcal{T}_n|$ in NOCGT-MAS scheme decreases as the channel gain threshold increases, it can be seen from (19) and (23) that, both the data transmission rate and feedback rate decrease with the increase of the channel gain threshold. However, the fading speed of feedback rate is much higher than that of data transmission rate when the threshold is sufficiently low, which makes the effective throughput raises first. With the improvement of channel gain threshold, the descent speed of data transmission rate gradually exceeds that of feedback rate, resulting in the decrease in the effective throughput. Finally, when the threshold is sufficiently high, no antenna can be selected for transmission and the effective throughput decreases to zero. The conclusions mentioned above are similar as the results given in Fig. 1, showing the existence of an optimal effective throughput of NOCGT-MAS scheme. To solve this optimization problem, we propose two algorithms named OICGT-MAS and OACGT-MAS.

A. An Optimal Instantaneous CGT-MAS Iterative Algorithm

In this subsection, we focus on the maximization of the instantaneous effective throughput of NOCGT-MAS scheme in a single time slot.

Based on the description above, the optimization problem can be formulated as

$$\begin{aligned} &\max_{I_j^k} C_T^{\text{MAS},k} \\ &s.t. \left|h_{id}^k\right|^2 > \alpha, A_i^k \in \mathcal{T}_n^k \\ &\quad \left|h_{id}^k\right|^2 \le \alpha, A_i^k \in \bar{\mathcal{T}}_n^k \\ &\quad \alpha \ge 0 \\ &\quad \alpha \in I_j^k, j = 1, 2, \ldots, M+1 \end{aligned} \tag{24}$$

where k represents the kth time slot and I_j^k represents the jth channel gain interval.

It can be observed from (24) that the optimization problem is nonlinear and complex. According to (23), we can conclude that the instantaneous effective throughput optimization objective is a piecewise function which is complex. Meanwhile, considering that the optimization variable I_j^k is not directly reflected in the mathematical expression of the optimization objective in (24), the change of the I_j^k impacts the number of selected antennas, and thus indirectly affects the effective throughput, making it a nonlinear optimization problem without a closed-form solution. However, the optimal interval can be located by numerical computer simulations. Consequently, we propose the OICGT-MAS iterative algorithm shown in Algorithm 1, where the optimal threshold interval can be found by numerical computer simulations. To be specific, Algorithm 1 first selects all the antennas with channel gain not less than the zth largest channel gain for transmission. Noting that $z = 1, \ldots, M$, we can obtain M

Algorithm 1: Optimal ICGT-MAS Iterative Algorithm.

Initialization: $\mathcal{T}_n^k = \phi$, $g_0^k = 0$, $g_{M+1}^k = \infty$, and $g_i^k = |h_{id}^k|^2$.
Sort g_i^k by size into $\mathbf{g}^k = \{g_0^k, \ldots, g_j^k, \ldots, g_{M+1}^k\}$, $g_{j-1}^k \le g_j^k, j = 1, \ldots, M+1$.
Set $I_j^k = [g_{j-1}^k, g_j^k)$ as the jth interval.
for:$j = 1 : M+1$, **do**
Select antenna A_i^k using $|h_{id}^k|^2 > g_j^k, A_i^k \in \mathcal{T}_n^k$.
Update $\mathcal{T}_n^k$.
Quantize h_{id}^k, $A_i^k \in \mathcal{T}_n^k$.
Compute $C_{T,j}^{\text{MAS},k}$.
end
Output: $I_{\text{opt}}^k = \arg\max_{I_j^k} C_{T,j}^{\text{MAS},k}$ and $C_{T,\max}^{\text{MAS},k} = \max C_{T,j}^{\text{MAS},k}$.

antenna selection results, and then calculate M different effective throughput values, of which the largest one is the optimal value of Algorithm 1. The corresponding left-end point of the optimal channel gain threshold interval is the maximal channel gain among unselected antennas, and the right-end point is the minimal channel gain among selected antennas. Considering that the OICGT-MAS iterative algorithm is a kind of exhaustive search method, its output can be considered as the optimal one.

B. An Optimal Average CGT-MAS Iterative Algorithm

In this subsection, we focus on the maximization of the average effective throughput of NOCGT-MAS scheme.

When N_c is very big, the quantization error σ_e^2 is negligible. At this time, for the case $|\mathcal{T}_n| > 1$, we can conclude that the data transmission rate can be further expressed as

$$C_d^{\text{MAS}}\left(|T_n| > 1\right) = B_c \log_2\left(1 + \gamma_s \sum_{A_i \in \mathcal{T}_n} |h_{id}|^2\right). \quad (25)$$

Combining (25) and (21), we can yield

$$\begin{aligned} E(C_T^{\text{MAS}}) &= \sum_{m=1}^{M} \Pr\left(|T_n| = m\right) E[C_T^{\text{MAS}}\left(|T_n| = m\right)] \\ &= \Pr\left(|T_n| = 1\right) E\left[C_T^{\text{MAS}}\left(|T_n| = 1\right)\right] \\ &\quad + \sum_{m=2}^{M} \Pr\left(|T_n| = m\right) E\left[C_T^{\text{MAS}}\left(|T_n| = m\right)\right]. \end{aligned} \quad (26)$$

Since that RVs h_{id} are i.i.d. with zero mean and variance σ_d^2 in Rayleigh model, for $m \in \{0, \ldots, M\}$, we have

$$\Pr\left(|T_n| = m\right) = \binom{M}{m}\left[\exp\left(-\frac{\alpha}{\sigma_d^2}\right)\right]^m \left[1 - \exp\left(-\frac{\alpha}{\sigma_d^2}\right)\right]^{M-m} \quad (27)$$

where $\binom{M}{m} = \frac{M!}{(M-m)!m!}$ and

$$E\Big(\sum_{A_i \in \mathcal{T}_n} |h_{id}|^2\Big) = |\mathcal{T}_{\text{n}}|(\alpha + \sigma_d^2). \quad (28)$$

The derivation of (28) is given in Appendix B.

Considering the approximation of $\log_2(1+x) \approx x\log_2 e$ when x is very small and combining (25), we can further express the data transmission rate at the very low SNR and high N_c region as

$$C_d^{\text{MAS}} \approx \begin{cases} B_c\gamma_s \sum\limits_{A_i \in \mathcal{T}_n} |h_{id}|^2 \log_2 e, & |\mathcal{T}_n| > 1 \\ B_c\gamma_s |h_{sd}|^2 \log_2 e, & |\mathcal{T}_n| = 1 \\ 0, & \mathcal{T} = \phi. \end{cases} \quad (29)$$

Hence, from (28) and (29), we can further obtain

$$\begin{aligned} E\left[C_d^{\text{MAS}}\left(|T_n| = 1\right)\right] &= E[B_c \log_2(1 + \gamma_s |h_{sd}|^2)] \\ &\approx B_c\gamma_s E(|h_{sd}|^2)\log_2 e \\ &= B_c\gamma_s(\alpha + \sigma_d^2)\log_2 e \end{aligned} \quad (30)$$

and

$$\begin{aligned} E\left[C_d^{\text{MAS}}\left(|T_n| = m\right)\right] &= E[B_c \log_2(1 + \gamma_s \sum_{A_i \in \mathcal{T}_n} |h_{id}|^2)] \\ &\approx B_c\gamma_s E\left(\sum_{A_i \in \mathcal{T}_n} |h_{id}|^2\right)\log_2 e \\ &= B_c\gamma_s m(\alpha + \sigma_d^2)\log_2 e. \end{aligned} \quad (31)$$

Substituting (27), (30), and (31) into (26), the average effective throughput can be further expressed as (32), shown at bottom of the next page.

Hence, the optimization problem can be formulated as

$$\begin{aligned} &\max_{\alpha} E(C_T^{\text{MAS}}) \\ &s.t.\, \alpha \ge 0. \end{aligned} \quad (33)$$

It can be observed from (32) and (33) that the optimization objective is nonlinear and complex, leading to the challenge of figuring out the closed-form solution of the channel gain threshold α. When it is challenging to calculate the derivative, golden section search is regarded as an efficient algorithm for finding out the extreme of an objective function with unimodal [31]. Motivated by this, we proposed a heuristic searching algorithm named OACGT-MAS iterative algorithm listed in Algorithm 2 based on the one-dimensional golden section search method to find the local optimum value by numerical computer simulations. The simulation results of the average effective throughput versus the number of iterations are given in Fig. 3 to show the convergence of OACGT-MAS algorithm. It can be

Algorithm 2: Optimal ACGT-MAS Iterative Algorithm.

Initialization: ε, $t = 0$, $t_{\max}$, $r = \frac{\sqrt{5}-1}{2}$, a^0, b^0, $\alpha_1^0 = b^0 - r(b^0 - a^0)$ and $\alpha_2^0 = a^0 + r(b^0 - a^0)$.
Repeat:
Calculate (32) with α_1^t and α_2^t respectively to obtain the corresponding $E(C_{T,1}^{\text{MAS}})$ and $E(C_{T,2}^{\text{MAS}})$.
If $E(C_{T,1}^{\text{MAS}}) \le E(C_{T,2}^{\text{MAS}})$, update $a = \alpha_1^t$, $\alpha_1^{t+1} = \alpha_2^t$, and $\alpha_2^{t+1} = a^{t+1} + r(b^{t+1} - a^{t+1})$.
else update $b^{t+1} = \alpha_2^t$, $\alpha_2^{t+1} = \alpha_1^t$, and $\alpha_1^{t+1} = b^{t+1} - r(b^{t+1} - a^{t+1})$.
$t = t + 1$.
Until: $|b^t - a^t| \le \varepsilon$ or $t \ge t_{\max}$
Output: $E[C_T^{\text{MAS}}(\alpha_{\text{opt}})]$ and $\alpha_{\text{opt}} = \frac{(a^t + b^t)}{2}$.

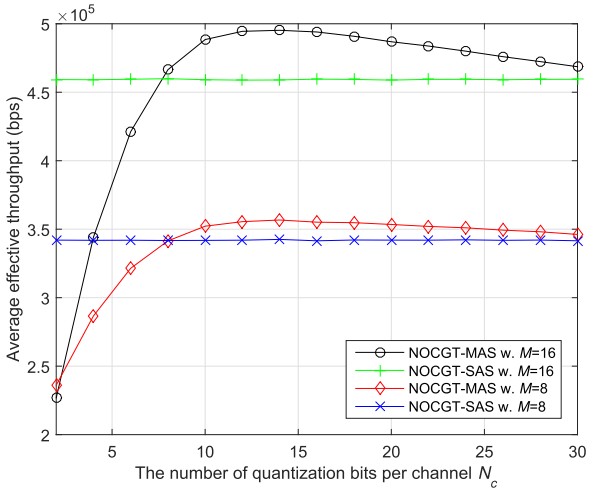

Fig. 6. Average effective throughput versus the number of quantization bits per channel N_c of NOCGT-MAS and NOCGT-SAS schemes for different number of total transmit antennas M with the bandwidth $B_c = 100$ kHz, the number of feedback bits per channel $N_c = 16$, the SNR $\gamma_s = 10$ dB, and the channel gain $\sigma_{id}^2 = 1$.

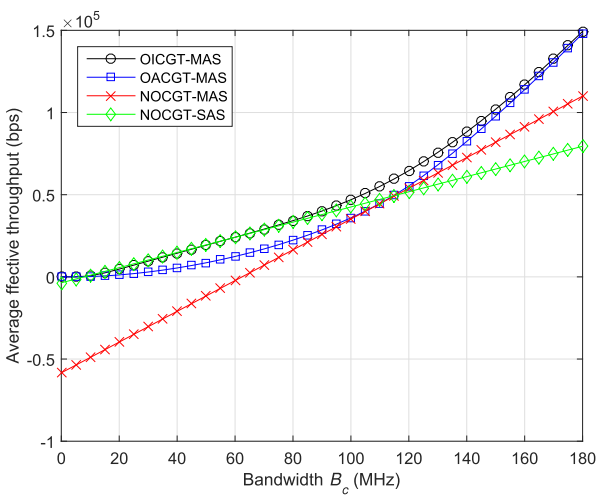

Fig. 7. Average effective throughput versus bandwidth B_c of OICGT-MAS, OACGT-MAS, NOCGT-MAS, and NOCGT-SAS schemes with the number of total transmit antennas $M = 16$, the number of feedback bits per channel $N_c = 24$, the SNR $\gamma_s = -40$ dB, and the channel gain $\sigma_{id}^2 = 1$.

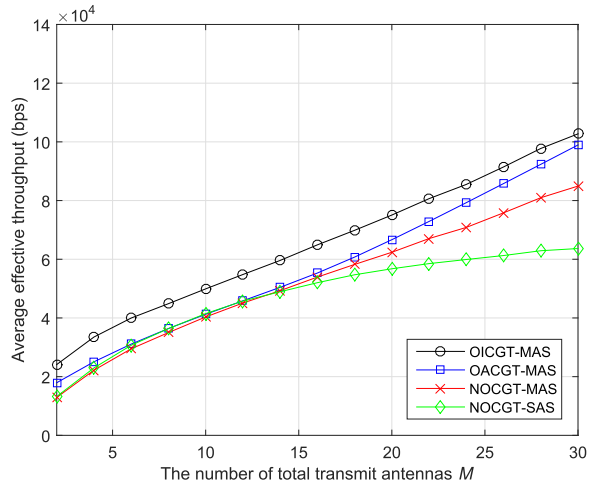

Fig. 8. Average effective throughput versus the number of total transmit antennas M of OICGT-MAS, OACGT-MAS, NOCGT-MAS, and NOCGT-SAS schemes with the bandwidth $B_c = 120$ MHz, the number of feedback bits per channel $N_c = 24$, the SNR $\gamma_s = -40$ dB, and the channel gain $\sigma_{id}^2 = 1$.

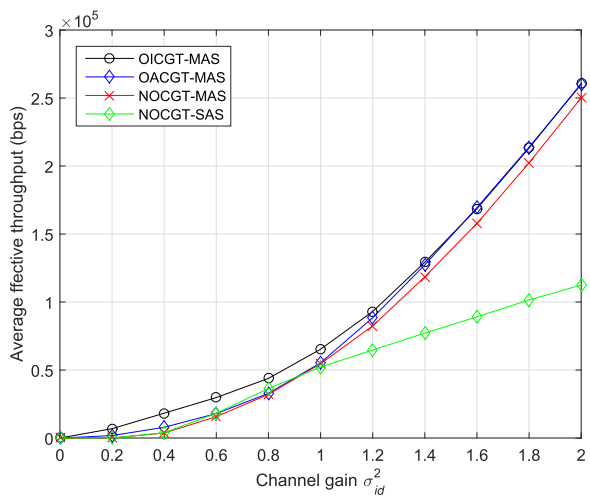

Fig. 9. Average effective throughput versus channel gain σ_{id}^2 of OICGT-MAS, OACGT-MAS, NOCGT-MAS, and NOCGT-SAS schemes with the bandwidth $B_c = 120$ MHz, the number of total transmit antennas $M = 16$, the number of quantization bits per channel $N_c = 24$, and the SNR $\gamma_s = -40$ dB.

observed from Fig. 3 that, as the number of iterations increases, the average effective throughput obtained by OACGT-MAS algorithm gradually converges.

It can be observed from Algorithm 1 that the OICGT-MAS iterative algorithm aims at maximizing the instantaneous effective throughput in each single time slot by adjusting the corresponding optimal transmission subset of the selected antennas according to different instantaneous CSI in different time slots. By contrast, the OACGT-MAS iterative algorithm shown in Algorithm 2 provides a specific local optimal threshold value to maximize the average effective throughput, where only the statistical CSI is employed. Thus, the average effective throughput of OICGT-MAS algorithm performs better, as shown in Figs. 7–9, since that the OICGT-MAS algorithm can realize more accurate adaptive antenna selection via utilizing the instantaneous CSI in different time slots. Nevertheless, the optimal

$$E(C_T^{\mathrm{MAS}}) = M\exp\left(-\frac{\alpha}{\sigma_d^2}\right)\left[1-\exp\left(-\frac{\alpha}{\sigma_d^2}\right)\right]^M\left\{B_c\gamma_s(\alpha+\sigma_d^2)\log_2 e - \frac{\log_2 M+1}{T_c}\right\}$$
$$+\sum_{m=2}^{M}\binom{M}{m}\left[\exp\left(-\frac{\alpha}{\sigma_d^2}\right)\right]^m\left[1-\exp\left(-\frac{\alpha}{\sigma_d^2}\right)\right]^{M-m}\left\{B_c\gamma_s m(\alpha+\sigma_d^2)\log_2 e - \frac{mN_c+\log_2(2^M-1-M)+1}{T_c}\right\} \quad (32)$$

interval for different time slots may be different, causing that neither an unchanged optimal interval nor a general threshold value can be given in the OICGT-MAS algorithm, while the OACGT-MAS algorithm can provide a certain threshold with lower complexity at the cost of the performance of average effective throughput. Specifically, noting that Algorithm 1 is performed in a single time slot, we need to calculate M times to obtain different effective throughput values by selecting all the antennas with channel gain not less than the zth largest channel gain, $z = 1, \ldots, M$, compare the M values to select the largest one, and repeat K times to compute the average value of effective throughput for K time slots. However, considering that the results of Algorithm 2 are the same in different time slots because the average effective throughput from (32) does not under the effect of instantaneous CSI, we only need N iterations where the average effective throughput needs to be calculated twice for comparison in every iteration. Hence, Algorithm 1 needs to calculate the effective throughput a total of MK times, while Algorithm 2 only needs to calculate $2N$ times. Due to the fact that K needs to be set as a very big value to make sure the Monte–Carlo simulation result is sufficiently reliable, the number of iterations required for convergence N is much less than K. Meanwhile, $M \geq 2$. Thus, the OICGT-MAS scheme achieves higher performance at the cost of complexity.

V. Simulation Results

In this section, we present numerical simulations to show the effective throughput of OICGT-MAS, OACGT-MAS, NOCGT-MAS, and NOCGT-SAS schemes. Besides, the analysis for simulation results is also shown in this section. In our simulation, unless otherwise stated, we consider the RVs h_{id} are i.i.d. with zero mean and variance $\sigma_{id}^2 = 1$, where $i \in \{1, 2, \ldots\ldots, M\}$, and we set $T_c = 1$ ms as the coherence time and $M = 16$ as the number of total transmit antennas at source.

Fig. 4 illustrates the average effective throughput versus the channel gain threshold α of NOCGT-MAS and NOCGT-SAS schemes with different number of total transmit antennas M. It can be seen from Fig. 4 that with the improvement of threshold α, the average effective throughput of NOCGT-MAS scheme increases initially, then decreases, showing the existence of an optimal threshold, which is consistent with our analysis in Section IV. However, the average effective throughput of NOCGT-SAS scheme fades slowly at first and then reduces fast, as the threshold increasing. This is because that the probability of $|h_{sd}|^2 > \alpha$ goes to 1 with sufficiently low α, and then gradually decreases as α continued increasing. Besides, when α is sufficiently high ($\alpha > 3$ in Fig. 4), the curves of average effective throughput for both schemes gradually coincide with each other, which indicates that the favorable effect of α on NOCGT-MAS scheme is negligible with sufficiently large channel gain threshold and the probability of outage event $\Pr(|T_n| = 0)$ grows. With α continued increasing, the effective throughput gradually converges to 0, showing that the probability of outage event tends to 1.

It can also be observed from Fig. 4 that the NOCGT-MAS scheme always performs better than the NOCGT-SAS scheme, except for the situation that α is sufficiently low, showing the superiority of our proposed NOCGT-MAS scheme. The inferior position of NOCGT-MAS scheme is because that the feedback rate of NOCGT-MAS scheme is much higher when α is very small. Moreover, as M increases from 8 to 16, the average effective throughput increases at the same time, demonstrating the positive effect of M.

Fig. 5 depicts the average effective throughput versus SNR γ_s of NOCGT-MAS and NOCGT-SAS schemes for different channel gain threshold α. In Fig. 5, with the development of γ_s, the average effective throughput curves of both NOCGT-MAS and NOCGT-SAS schemes all improve, showing the positive effect of γ_s. Meanwhile, when γ_s is within the normal range, the performance of NOCGT-MAS scheme is better than that of NOCGT-SAS scheme. It should be pointed out that, when $|\mathcal{T}_n| = 1$, no performance floor occurs since that no interference exists as shown in (12) and (20). However, when $|\mathcal{T}_n| > 1$, the average effective throughput with high SNR will converge to the floor due to the existence of the interference caused by channel quantization, as shown in (20) and (21). Accordingly, it can be observed from Fig. 5 that the performance of NOCGT-SAS scheme increases as γ_s increases, while the growth rates of the curves for NOCGT-MAS scheme decrease with SNR increasing to a high level. Besides, the performance of NOCGT-SAS scheme with $\alpha = 1$ is higher than that with $\alpha = 2$, and the performance of NOCGT-MAS scheme with $\alpha = 1$ also achieves a higher performance when γ_s is within the normal range, which are consistent with the simulation results from Fig. 4.

It also can be observed from Fig. 5 that, in the high-SNR region, the average effective throughput of NOCGT-MAS scheme with $\alpha = 1$ converges to a floor at last while that of NOCGT-MAS scheme with $\alpha = 2$ continues to increase at a lower growth rate. This is because that the probability of $|\mathcal{T}_n| > 1$ is almost one with $\alpha = 1$, where the performance floor occurs. However, the probability of $|\mathcal{T}_n| > 1$ decreases and the effective throughput of the case $|\mathcal{T}_n| = 1$ continued increasing with a much higher value as γ_s increases when $\alpha = 2$, making the average effective throughput value dominated by the case $|\mathcal{T}_n| = 1$. Accordingly, when γ_s increases to a high region, the average effective throughput of NOCGT-SAS scheme will outperform that of NOCGT-MAS scheme, and the performance of NOCGT-MAS with $\alpha = 2$ is better.

Fig. 6 illustrates the average effective throughput versus the number of quantization bits per channel N_c of NOCGT-MAS and NOCGT-SAS schemes for different number of total transmit antennas M, where we set $\alpha = 2$. It needs to be pointed out that, with $M = 16$, the optimal value of α is near 1 and the favorable effect of α on NOCGT-MAS scheme is negligible when $\alpha > 3$ as shown in Fig. 4. Thus, we set $\alpha = 2$ to analyze the differences between NOCGT-MAS scheme and NOCT-SAS scheme in Fig. 6. It can be seen from Fig. 6 that, with the improvement of N_c, the average effective throughput of NOCGT-SAS remains unchanged, since that the quantization is not employed. Fig. 6 also plots that, as N_c rising up, the average effective throughput of NOCGT-MAS scheme rapidly increases first and then decreases gradually. This is because that the enhancement of data transmission rate when $|\mathcal{T}_n| > 1$, which is caused by the improvement of quantization accuracy, is at the cost of the increase of feedback overhead. To be specific, when N_c increases initially from 0, the increases of data transmission rate affected by the obviously reduce of quantization error is significantly higher than that of the feedback rate, which accounts for the initial improvement of the effective throughput. While N_c continued increasing to a certain range, the improvement of quantization accuracy is negligible, which makes the data transmission rate reach limitation as feedback rate significantly increases, further causing the decrease.

It also can be observed from Fig. 6 that, with the growth of N_c, the effective throughput of the NOCGT-MAS scheme gradually changes from lower to higher than that of NOCGT-SAS scheme. Noting that the improvement of quantization accuracy has more positive effect on the data transmission rate than feedback rate as N_c increases, the data transmission rate achieves a higher improvement, which causes the enhancement of average effective throughput of NOCGT-MAS scheme. Moreover, there exists an optimal N_c for NOCGT-MAS scheme, showing an optimization problem for our future research.

Fig. 7 plots the average effective throughput versus bandwidth B_c of OICGT-MAS, OACGT-MAS, NOCGT-MAS, and NOCGT-SAS schemes, where we set $\alpha = 2$ for two nonoptimized schemes. As shown in Fig. 7, all these four schemes achieve an increased average effective throughput as B_c increases, showing the positive effect of B_c. Meanwhile, the effective throughput performance of NOCGT-MAS scheme has changed from worse to better than that of NOCGT-SAS scheme as B_c increases. The reason behind the worse performance is that the negative impact of feedback overhead is greater for NOCGT-MAS. As B_c increases, the advantage of the data transmission rate gradually changes from lower to higher than the disadvantage of the feedback rate of NOCGT-MAS scheme over NOCGT-SAS scheme. To the end, when B_c improves to a certain range, the average effective throughput of NOCGT-MAS scheme gradually surpasses that of NOCGT-SAS scheme, and the advantage expands as B_c continued increasing. Besides, there exists negative values of both NOCGT-MAS and NOCGT-SAS schemes, since that the feedback rate is larger than data transmission rate when B_c is not big enough.

It also can be observed from Fig. 7 that, with the growth of B_c, the advantage of OACGT-MAS scheme over NOCGT-MAS scheme with $\alpha = 2$ decreases first and then increases, which demonstrates that the local optimal channel gain threshold value gradually approaches to 2 and then moves away. We can also observe from Fig. 7 that the OICGT-MAS performs better than OACGT-MAS in terms of average effective throughput. Furthermore, when B_c is sufficiently large, the advantage of OICGT-MAS is very small, which means that the OACGT-MAS can achieve a close average effective throughput performance to the OICGT-MAS while providing a general average-threshold value and less computation.

Fig. 8 shows the average effective throughput versus the number of total transmit antennas M of OICGT-MAS, OACGT-MAS, NOCGT-MAS, and NOCGT-SAS schemes, where we set $\alpha = 2$ for two nonoptimized schemes. As shown in Fig. 8, with the improvement of M, the four schemes all achieve an increased average effective throughput, showing the positive effect of M. However, the growth of the average effective throughput of NOCGT-SAS scheme gradually slows down while that of other three schemes continued increasing fast. This is because that the possible maximal number of active antennas is only 1, making the improvement of the average effective throughput of NOCGT-SAS scheme limited. Besides, the performance of NOCGT-MAS scheme changes from worse to better than that of NOCGT-SAS scheme with $\alpha = 2$. The reason for the worse performance of NOCGT-MAS scheme is that, compared with NOCGT-SAS scheme where only one optimal antenna can be selected for transmission, the negative impact of the feedback rate is much higher than the increase of data transmission rate as the number of selected antennas increases for NOCGT-MAS scheme when M is small. As M continued increases, the improvement of the data transmission rate is much higher than that of feedback rate of NOCGT-MAS scheme, causing its effective throughput gradually become higher.

Fig. 8 also demonstrates that, as the number of total transmit antennas M increases, the advantage of OACGT-MAS scheme over the NOCGT-MAS scheme in terms of average effective throughput decreases first and then increases, indicating that the local optimal threshold value is gradually close to and then away from 2. Meanwhile, the average effective throughput of OICGT-MAS scheme performs better than that of OACGT-MAS scheme, further demonstrating that the OICGT-MAS scheme can achieve higher performance. Besides, it can be observed from Fig. 8 that, as M increases, the gap between the average effective throughput of OICGT-MAS scheme and that of OACGT-MAS scheme gradually decreases, indicating that when M is sufficiently large, OACGT-MAS scheme can achieve the similar performance to OICGT-MAS scheme.

Fig. 9 depicts the average effective throughput versus channel gain σ_{id}^2 of OICGT-MAS, OACGT-MAS, NOCGT-MAS, and NOCGT-SAS schemes, where we set $\alpha = 2$ for two nonoptimized schemes. One can be seen from Fig. 9 that, with the channel fading variance σ_{id}^2 increasing, the average effective throughput improves, reflecting the positive effect of σ_{id}^2 on the average effective throughput. One can also be seen from Fig. 9 that, as σ_{id}^2 increases to a certain range, NOCGT-MAS scheme performs better than NOCGT-SAS scheme and the more advantage can be achieved in terms of the average effective throughput, since that the improvement of σ_{id}^2 leads to higher instantaneous channel gain, showing more favorable influence of σ_{id}^2 on NOCGT-MAS scheme. However, when σ_{id}^2 is in a small region, the performance of NOCGT-SAS scheme is better than that of NOCGT-MAS scheme. This is because that the advantage of data transmission rate of NOCGT-MAS scheme over NOCGT-SAS scheme is lower than the disadvantage of feedback rate when σ_{id}^2 is in small region, making the effective throughput performance worse.

It also can be observed from Fig. 9 that, as σ_{id}^2 increases, the advantage of OACGT-MAS scheme over NOCGT-MAS scheme decreases first and then increases. This demonstrates that the local optimal threshold value comes closer and then goes away from 2. Besides, the OICGT-MAS scheme performs better than OACGT-MAS scheme, and the advantage of the average effective throughput of OICGT-MAS scheme over OACGT-MAS scheme decreases to negligible with the improvement of σ_{id}^2, further showing the substitutability of OACGT-MAS.

VI. Conclusion

In this article, we considered a downlink wireless communication system with a multiantenna base station in face of limited feedback. We proposed the NOCGT-MAS scheme to choose those antennas with relatively good channel quality, while the remaining transmit antennas failing to meet a given channel quality requirement are inactivated. The conventional NOCGT-SAS scheme was considered as baseline, where only the single transmit antenna with the highest channel gain exceeding a predefined threshold is employed for transmitting signals. We provided the analysis of effective throughput defined as the difference between the data transmission rate and feedback rate for both nonoptimized schemes. We found that an optimal threshold exists to maximize the effective throughput

of NOCGT-MAS scheme. To this end, we proposed OICGT-MAS algorithm to maximize instantaneous effective throughput. Besides, we provided the derivation of the closed-form expression of an average effective throughput for the CGT-MAS and proposed the OACGT-MAS algorithm to maximize the average effective throughput. Numerical results showed that the proposed NOCGT-MAS performs better than the NOCGT-SAS in terms of the effective throughput. It was also shown from the simulation results that the existence of the optimal threshold is consistent with our analysis. Moreover, the OICGT-MAS achieves a higher effective throughput than OACGT-MAS at the cost of computational complexity.

APPENDIX A
DERIVATIONS OF (2), (4), AND (5)

As mentioned in our previous work [1], the probability that either the real part $\mathrm{Re}(h_{id})$ or the imaginary part $\mathrm{Im}(h_{id})$ denoted by h_x falls below the lth quantization level d_l in the EPQ is $\Pr(h_x < d_l) = \frac{l}{N_q}$, $l \in \{0, 1, \ldots, N_q\}$. Meanwhile, it is assumed that RV h_x follows the Gaussian distribution with zero mean and variance $\sigma_{id}^2/2$, we can obtain

$$\begin{aligned}\Pr(h_x < d_l) &= \int_{-\infty}^{d_l} \frac{1}{\sqrt{\pi}\sigma_{id}} \exp\left(-\frac{x^2}{\sigma_{id}^2}\right) dx \\ &= 1 - Q\left(\frac{\sqrt{2}}{\sigma_{id}} d_l\right). \end{aligned} \tag{A.1}$$

Thus, we have $\frac{l}{N_q} = 1 - Q(\frac{\sqrt{2}}{\sigma_{id}} d_l)$, from which (2) is concluded.

When h_x falls between d_{l-1} and d_l, we can yield $\Pr(h_x < q_l) = \frac{1}{2}(\frac{l-1}{N_q} - \frac{l}{N_q}) = \frac{2l-1}{2N_q}$, where q_l is the corresponding quantized value, $l \in \{1, \ldots, N_q\}$. Meanwhile, we have

$$\begin{aligned}\Pr(h_x < q_l) &= \int_{-\infty}^{q_l} \frac{1}{\sqrt{\pi}\sigma_{id}} \exp\left(-\frac{x^2}{\sigma_{id}^2}\right) dx \\ &= 1 - Q\left(\frac{\sqrt{2}}{\sigma_{id}} q_l\right). \end{aligned} \tag{A.2}$$

Hence, we obtain $\frac{2l-1}{2N_q} = 1 - Q(\frac{\sqrt{2}}{\sigma_{id}} q_l)$, from which (4) is concluded.

Letting X_i denote h_x, $x \in (-\infty, \infty)$, and denoting the quantized value of X_i by $q(X_i)$, the channel quantization error variance of X_i is given by

$$\begin{aligned}\sigma_{X_i}^2 &= E\left(|X_i - q(X_i)|^2\right) \\ &= \sum_{l=1}^{N_q} \int_{d_{l-1}}^{d_l} \frac{(x - q_l)^2}{\sqrt{\pi}\sigma_{id}} \exp\left(-\frac{x^2}{\sigma_{id}^2}\right) dx \end{aligned} \tag{A.3}$$

which is further expressed as $\sigma_{X_i}^2 = 2\sum_{l=1}^{N_q} \Phi_l$, where

$$\Phi_l = \int_{d_{l-1}}^{d_l} \frac{(x - q_l)^2}{\sqrt{\pi}\sigma_{id}} \exp\left(-\frac{x^2}{\sigma_{id}^2}\right) dx \tag{A.4}$$

from which (5) is concluded.

APPENDIX B
DERIVATION OF (28)

Denoting $Y_i = |h_{id}|^2$, $i = 1, 2, \ldots, M$, since that the RVs $|h_{id}|^2$ follow the exponential distribution and are i.i.d. with mean σ_d^2, the probability density function of Y_i is given by

$$f_{Y_i}(y) = \begin{cases} \frac{1}{\sigma_d^2} e^{-\frac{y}{\sigma_d^2}}, & y > 0 \\ 0, & y \le 0. \end{cases} \tag{B.1}$$

Combining the antenna selection criterion given in (6), we obtain the expectation of Y_j, $A_j \in \mathcal{T}_n$ as

$$\begin{aligned}E(Y_j) &= E(Y_j | Y_j > \alpha) \\ &= \frac{\int_\alpha^\infty y f_{Y_j}(y) dx}{\int_\alpha^\infty f_{Y_j}(y) dy} \\ &= \alpha + \sigma_d^2. \end{aligned} \tag{B.2}$$

Denoting $Z = \sum_{A_j \in \mathcal{T}_n} |h_{jd}|^2$, we have

$$\begin{aligned}E(Z) &= E(\sum_{A_j \in \mathcal{T}_n} Y_j | Y_j > \alpha, \forall A_j \in \mathcal{T}_\mathrm{n}) \\ &= \sum_{A_j \in \mathcal{T}_n} E(Y_j | Y_j > \alpha). \end{aligned} \tag{B.3}$$

Substituting (B.2) into (B.3), we conclude

$$E\left(\sum_{A_i \in \mathcal{T}_n} |h_{id}|^2\right) = |\mathcal{T}_\mathrm{n}|(\alpha + \sigma_d^2). \tag{B.4}$$

REFERENCES

[1] Y. Zou, "Precoding design and optimization for multi-antenna systems with limited feedback," *IEEE Trans. Veh. Technol.*, vol. 69, no. 7, pp. 7306–7316, Jul. 2020.

[2] J. G. Andrews *et al.*, "What will 5G be," *IEEE J. Sel. Areas Commun.*, vol. 32, no. 6, pp. 1065–1082, Jun. 2014.

[3] M. Jaber, M. A. Imran, R. Tafazolli, and A. Tukmanov, "5G backhaul challenges and emerging research directions: A survey," *IEEE Access*, vol. 4, pp. 1743–1766, Apr. 2016.

[4] Y. Liu, H. Chen, and L. Wang, "Physical layer security for next generation wireless networks: Theories, technologies, and challenges," *IEEE Commun. Surv. Tut.*, vol. 19, no. 1, pp. 347–376, Jan.–Mar. 2017.

[5] E. G. Larsson, O. Edfors, F. Tufvesson, and T. L. Marzetta, "Massive MIMO for next generation wireless systems," *IEEE Commun. Mag.*, vol. 52, no. 2, pp. 186–195, Feb. 2014.

[6] Z. Chen, L. Qiu, and X. W. Liang, "Area spectral efficiency analysis of multi-antenna two-tier cellular networks," *IEEE Commun. Lett.*, vol. 21, no. 1, pp. 108–111, Jan. 2017.

[7] W. Li and M. Dong, "Joint relay beamforming and receiver processing for multi-way multi-antenna relay networks," *IEEE Trans. Commun.*, vol. 66, no. 2, pp. 576–588, Feb. 2018.

[8] T. Nguyen and B. An, "Cognitive multihop wireless powered relaying networks over Nakagami-m fading channels," *IEEE Access*, vol. 7, pp. 154600–154616, Oct. 2019.

[9] Y. Cao *et al.*, "Secrecy analysis for cooperative NOMA networks with multi-antenna full-duplex relay," *IEEE Trans. Commun.*, vol. 67, no. 8, pp. 5574–5587, Aug. 2019.

[10] H. Yang, B. Li, G. Liu, and R. Ma, "Physical-layer network coding based multi-user cooperative relay transmission with multi-antennas in cognitive wireless networks," *IEEE Access*, vol. 6, pp. 40189–40197, Jul. 2018.

[11] M. Li, H. Yin, Y. Huang, Y. Wang, and R. Yu, "The security of cognitive multiuser networks over space-and-time correlated channels," *IEEE Syst. J.*, vol. 13, no. 3, pp. 2806–2817, Sep. 2019.

[12] M. Bacha, Y. Wu, and B. Clerckx, "Downlink and uplink decoupling in two-tier heterogeneous networks with multi-antenna base stations," *IEEE Trans. Wireless Commun.*, vol. 16, no. 5, pp. 2760–2775, May 2017.
[13] D. C. Gonzalez, D. B. da Costa, and J. C. S. Santos Filho, "Distributed TAS/MRC and TAS/SC schemes for fixed-gain AF systems with multiantenna relay: Outage performance," *IEEE Trans. Wireless Commun.*, vol. 15, no. 6, pp. 4380–4392, Jun. 2016.
[14] P. Shaik, P. K. Singya, and V. Bhatia, "On impact of imperfect CSI over hexagonal QAM for TAS/MRC-MIMO cooperative relay network," *IEEE Commun. Lett.*, vol. 23, no. 10, pp. 1721–1724, Oct. 2019.
[15] J. Si, Z. Li, J. Cheng, and C. Zhong, "Asymptotic secrecy outage performance for TAS/MRC over correlated Nakagami-m fading channels," *IEEE Trans. Commun.*, vol. 67, no. 11, pp. 7700–7714, Nov. 2019.
[16] V. Kumar, B. Cardiff, and M. F. Flanagan, "Performance analysis of NOMA with generalised selection combining receivers," *Electron. Lett.*, vol. 55, no. 25, pp. 1364–1367, Dec. 2019.
[17] B. S. Tan, K. H. Li, and K. C. Teh, "Performance study of transmit antenna selection with switch-and-examine combining over Rayleigh fading," *IEEE Trans. Veh. Technol.*, vol. 61, no. 9, pp. 4205–4211, Nov. 2012.
[18] M. Yang, B. Zhang, Y. Huang, D. Guo, and X. Yi, "Ergodic secrecy capacity for downlink multiuser networks using switch-and-examine combining with post-selection scheduling scheme," *Electron. Lett.*, vol. 52, no. 9, pp. 720–722, Apr. 2016.
[19] B. S. Tan, K. H. Li, and K. C. Teh, "Analysis of transmit antenna selection with output-threshold generalised selection combining over Rayleigh fading," *IET Commun.*, vol. 7, no. 15, pp. 1587–1595, 15 Oct. 2013.
[20] P. S. Bithas, A. A. Rontogiannis, and G. K. Karagiannidis, "An improved threshold-based channel selection scheme for wireless communication systems," *IEEE Trans. Wireless Commun.*, vol. 15, no. 2, pp. 1531–1546, Feb. 2016.
[21] R. Sarvendranath and N. B. Mehta, "Impact of multiple primaries and partial CSI on transmit antenna selection for interference-outage constrained underlay CR," *IEEE Trans. Wireless Commun.*, vol. 18, no. 2, pp. 942–953, Feb. 2019.
[22] Y. Zhang and R. S. Cheng, "Relay subset selection in cooperative systems with beamforming and limited feedback," *IEEE Trans. Wireless Commun.*, vol. 12, no. 10, pp. 5271–5281, Oct. 2013.
[23] A. Yilmaz and O. Kucur, "Performances of transmit antenna selection, receive antenna selection, and maximal-ratio-combining-based hybrid techniques in the presence of feedback errors," *IEEE Trans. Veh. Technol.*, vol. 63, no. 4, pp. 1976–1982, May 2014.
[24] J. Park, N. Lee, J. G. Andrews, and R. W. Heath, "On the optimal feedback rate in interference-limited multi-antenna cellular systems," *IEEE Trans. Wireless Commun.*, vol. 15, no. 8, pp. 5748–5762, Aug. 2016.
[25] M. Min, "Bounds on the optimal feedback rate for multi-antenna systems in interference-limited cellular networks," *IEEE Trans. Wireless Commun.*, vol. 17, no. 7, pp. 4845–4860, Jul. 2018.
[26] Z. Tang, L. Sun, L. Cao, S. Qi, and Y. Feng, "Reconsidering design of multi-antenna NOMA systems with limited feedback," *IEEE Trans. Wireless Commun.*, vol. 19, no. 3, pp. 1519–1534, Mar. 2020.
[27] S. K. Mishra and K. D. Kulat, "Reduced feedback rate schemes for transmit antenna selection with alamouti coding," *IEEE Access*, vol. 6, pp. 10028–10040, 2018.
[28] J. Choi *et al.*, "Base station antenna selection for low-resolution ADC systems," *IEEE Trans. Commun.*, vol. 68, no. 3, pp. 1951–1965, Mar. 2020.
[29] J. Zhu, Y. Yao, Y. Zou, and T. Wu, "Cooperative beamforming for multi-relay networks with limited feedback," *China Commun.*, vol. 16, no. 10, pp. 56–64, 2019.
[30] Y. Zou, B. Champagne, W. Zhu, and L. Hanzo, "Relay-selection improves the security-reliability trade-off in cognitive radio systems," *IEEE Trans. Commun.*, vol. 63, no. 1, pp. 215–228, Jan. 2015.
[31] Y.-C. Chang, "N-dimension golden section search: Its variants and limitations," in *Proc. Int. Conf. Biomed. Eng. Informat.*, 2009, pp. 1–6.

Tong Wu received the B.Eng. degree in broadcasting and television engineering, in 2016, from the Nanjing University of Posts and Telecommunications (NUPT), Nanjing, China, where she is currently working toward the Ph.D. degree in signal and information processing.

Her research interests include multiantenna system, transmit antenna selection, channel quantization, and physical-layer security.

Yulong Zou received the B.Eng. degree in information engineering from the Nanjing University of Posts and Telecommunications (NUPT), Nanjing, China, in 2006, the first Ph.D. degree in electrical engineering from the Stevens Institute of Technology, Hoboken, NJ, USA, in 2012, and the second Ph.D. degree in signal and information processing from the NUPT, in 2012.

He is currently a Full Professor and a Ph.D. Supervisor with the NUPT.

Dr. Zou was a Technical Program Committee Member of various IEEE-sponsored conferences, such as the IEEE ICC, GLOBECOM, WCNC, VTC, and ICCC. He was a recipient of the 9th IEEE Communications Society Asia-Pacific Best Young Researcher in 2014. He was a co-receipient of the Best Paper Award at the 80th IEEE Vehicular Technology Conference, in 2014. He was an Editor of the IEEE COMMUNICATIONS SURVEYS AND TUTORIALS, the IEEE COMMUNICATIONS LETTERS, the *EURASIP Journal on Advances in Signal Processing*, the *IET Communications*, and the *China Communications*.

Jia Zhu received the B.Eng. degree in computer science and technology from Hohai University, Nanjing, China, in 2005, and the Ph.D. degree in signal and information processing from the Nanjing University of Posts and Telecommunications, Nanjing (NUPT), Nanjing, China, in 2010.

From June 2010 to June 2012, she was a Postdoctoral Research Fellow with the Stevens Institute of Technology, Hoboken, NJ, USA. Since November 2012, she has been a full-time Faculty Member with the Telecommunication and Information School, NUPT, where she is currently a Full Professor. Her research interests include the cognitive radio, physical-layer security, and communications theory.

Hao Wei received the B.E. degree in electrical information engineering and M.E. degree in signal and information processing from the Nanjing University of Posts and Telecommunications, Nanjing, China, in 2010 and 2013, and the Ph.D. degree in information and communication engineering from Southeast University, Nanjing, China, in 2016.

He is currently with the State Key Laboratory of Mobile Network and Mobile Multimedia Technology, ZTE Corporation, Shenzhen, China, as a Senior Algorithm System Engineer, responsible for wireless communication products R&D. His interests include wireless communication and signal processing technologies.

George K. Karagiannidis (Fellow, IEEE) was born in Pithagorion, Samos Island, Greece. He received the University Diploma (5 years) and Ph.D. degrees in electrical and computer engineering from the University of Patras, Patras, Greece, in 1987 and 1999, respectively.

From 2000 to 2004, he was a Senior Researcher with the Institute for Space Applications and Remote Sensing, National Observatory of Athens, Greece. Since June 2004, he has been a Faculty with Aristotle University of Thessaloniki, Thessaloniki, Greece, where he is currently a Professor with the Electrical and Computer Engineering Department and the Head of Wireless Communications and Information Processing (WCIP) Group. He is also Honorary Professor with South West Jiaotong University, Chengdu, China. His research interests include digital communications systems and signal processing, with emphasis on wireless communications, optical wireless communications, wireless power transfer, and applications and communications and signal processing for biomedical engineering.

Dr. Karagiannidis has been a General Chair, Technical Program Chair, and Member of Technical Program Committees for several IEEE and non-IEEE conferences. He was an Editor of several IEEE journals, and from 2012 to 2015, he was the Editor-in Chief of the IEEE COMMUNICATIONS LETTERS. He is currently an Associate Editor-in Chief of the IEEE OPEN JOURNAL OF COMMUNICATIONS SOCIETY. He is one of the highly cited authors across all areas of electrical engineering, recognized from Clarivate Analytics as Web-of-Science Highly Cited Researcher in seven consecutive years 2015–2021.